Near-Infrared Raman Spectroscopy for Tissue characterisation: Adaption of the Set-up for Medical use.

Diploma Paper
by
Anders Åkesson

Lund Reports on Atomic Physics, LRAP-198
Lund, June 1996

1 Abstract

This work practically and theoretically evaluates the possibilities to use near infrared Raman spectroscopy for medical diagnosis. A set-up based on a diode laser, a fiberoptic probe, a single stage spectrometer and a CCD-detector was used to record spectra from liquid chemicals, pure tissue constitutes and tissue from pig heart.

The set-up used in this work is theoretically compared to a set-up consisting of the best available equipment and the improvement in performance was estimated. A medical background to atherosclerosis is also included, since diagnosis of this serious disorder probably is one of the most interesting application of such an optical biopsy technique.

2 Introduction

2.1 Introduction

As medical treatment of today is developing quickly to be more efficient, it is also often being more dependent on the ability to make an early and correct diagnosis. For several diseases, an early diagnosis is crucial to the efficiency and outcome of the medical treatment and in some cases it is even desirable to diagnose and treat simultaneously.

For tissue-diagnosis the traditional method is biopsy, in which a small amount of tissue is removed and examined in a laboratory. This method gives reliable and detailed results but unfortunately it has its drawbacks.Removal of tissue is a surgical operation. The area of interest can be difficult to reach, sensitive to surgery, or simply too delicate to be able to dispense even a small amount of tissue for laboratory tests. Obviously, there is a time delay between physical examination and completed diagnosis and since one has to choose small samples of tissue there is also a risk to obtain the only healthy part in a sick environment.

Among the methods developed as a complement to this indispensable but sometimes inconvenient way of tissue diagnosis, there are several techniques based on optical spectroscopy.These techniques use the fact that electromagnetic radiation ,light, which interacts with the atoms and molecules in an investigated material, can give information about its composition and structure. If the material is a tissue sample, it might be possible to identify different tissue types.

The interaction phenomenon used in this work is Raman-scattering. The Raman signal provides detailed information of the investigated material. Unfortunately, the probability for this type of scattering is small, which means that the signal to be measured is very weak.

Nevertheless previous work (Refs[1,2,3,4,5]) show that it is not only possible to perform Raman-spectroscopy on tissue, but also to distinguish between healthy and diseased tissue-samples.

An area of particular interest is the diagnosis of atherosclerosis. This common vascular disorder causes a raised plaque in the blood vessel which occludes the lumen and in the worst cases can lead to cerebral or cardiac infarction. One method to remove this obstacle is laser ablation. In this technique a large dose of energy is dumped in a small volume of tissue with a short laser pulse. The strong electrical field rips the molecules appart, disrupting cell and tissue structure, and dissolves the occlusion.

The use of spectroscopic diagnosis (for instance based on Raman spectroscopy) would not only increase the efficiency of the method significantly but also minimise the risk of unwanted vessel perforation. This risk to great extent limits the use of the technique today.

2.2 Spectroscopy- A Historical Background

By Spectroscopy we usually mean studying an object by analysing its electromagnetic radiation (light), dispersed in its different wavelength components (colours). Emission and absorption of light are closely connected to transitions between energy levels in atoms and molecules and hence spectroscopy usually is a way of mapping these energy levels. Since the obtained level scheme is not only characteristic of the substance (atom or molecule), but also reflects the surroundings (such as temperature, magnetic and electric fields). Thus spectroscopy provides analytical methods for both substances and their environment in a number of applications.

Natural spectral phenomenon like the northern light and rainbows must have fascinated man for thousands of years and probably this kind of spectacular optical effects helped creating the early scientific interest in light and it's properties. The astronomer Ptolemaeus described measurements and observations in refraction and optics as early as AD 130 and several other scientists (for instance Alhazen AD 1038) followed him. Despite this fascinating research, refraction and the nature of colours remained an elusive mystery for science for many years. Far into the 17:th century the prevalent idea was that white light changed into different colours within a refracting body (such as a prism or the water droplets producing the rainbow), and that colours were a mix of white and darkness.

In the early 17:th century Willeborn Snell discovered the law of refraction, but he as his predecessors did not distinguish between different colours. It was Isaac Newton who in 1704 took the first major step towards understanding of the true nature of light and colours, when he bought a glass prism "to try therewith the phenomena of colours" (Ref [6]). By letting sunlight from a round hole pass through the prism and fall on a screen, he recognised that the result was a series of coloured images of the entrance hole. He stated that "The Sun's light is a heterogeneous Mixture of Rays" and that in the prism they are "parted or sorted from one and other" (Ref [6]).

Unfortunately Newton falsely proposed that all light had the same nature and that different colours were caused by vibrations in the body that emitted them. Thus he turned his back on one of the great counterstones of spectroscopy, that emitted light is characteristic of the atom or molecule that produces it. His influence at this time was such that more than 150 years elapsed before this principle was pointed out and an other 50 before it was established.

Before that, several small, but important, observations and discoveries were made by a number of scientists, of which only a few will be mentioned here. In 1802 Thomas Young performed the first wavelength-determinations, and thereby established a way of international standard for comparing spectroscopic measurements.

During the first half of the 19:th century emission and absorption spectra from a variety of substances were measured and described by a number of different scientists. In 1814 Joseph Fraunhofer found that the solar spectrum was crossed with "an almost infinite number of strong and weak vertical lines" (Ref [7]).

These observations may seem unimportant one by one, but putting them all together G. R. Kirchoff in 1860 finally pointed out what could be regarded as the basic principles of spectroscopic analysis. He then described the connection between absorption and emission of light, and emphasised that emitted light is characteristic of the different elements.

He verified these two principles by using a gas flame containing common salt (Sodium-Chloride) and thus emitting the characteristic spectra of sodium. Kirchoff showed that the yellow lines of sodium were identical to a set of the dark lines that Fraunhofer had discovered in the sunlight, and that the sodium flame absorbed the same lines from a stronger source behind it. He went on to explain the dark Fraunhofer lines as absorption by the elements in the sun's cooler atmosphere of the continuos spectra emitted by the hotter interior of the sun (Ref [8]).

Thereby he showed the way for chemical analysis not only of the sun and shining stars, but also of other samples. Samples that did not emit light by themselves were analysed through interaction with light in a burner or electric discharge. As a result, the interest in spectroscopic studies arouse dramatically, all kinds of substances were analysed and new elements were discovered.

From here on the development of spectroscopy rapidly grow far beyond the possibilities and purpose of this brief chapter, but a few milestones on the way to today's techniques will be mentioned. Pretty soon scientists (for instance J R Rydberg and J J Balmer) started to seek a structure in the characteristic spectres of the elements, and they found that the arrangements of lines followed simple laws. This lead to Bohr's model of the hydrogen atom (1913) and finally the theory of quantum mechanics by Schrödinger and DeBroglie in 1925-1926.

As a result, the energy levels of atoms and molecules could be described and understood, and thus to great extent light interaction connected to transitions between them. The use of an external light source to introduce these transitions soon proved very successful, and for this purpose the development of the laser revolutionised spectroscopy in the 1960's. The number of new possible applications seems almost infinite and today they range from medical diagnostics to pollution monitoring and isotope separation.

A more complete introduction to Spectroscopy is found in Refs [9,10] and further reading about Isaac Newton in Ref [11].

2.3 This Project

As mentioned in the introduction, Raman-spectroscopy can be performed on tissue and thereby give information on the bio-chemical composition of a sample. By this information it is possible to draw medical conclusions, i.e. to use it for diagnostic purposes.

The purpose of this work is to take a further step towards a clinically usable set-up for vessel diagnosis, and evaluate the possibilities to develop such an equipment. This step includes the following main features:

* Briefly study the medical background and results of atherosclerosis. A general medical knowledge is surely helpful in order to develop diagnostic method for the disorder.

* Assemble a practical, Raman-spectroscopy set-up based on a cheap, easy to handlediode-laser, a flexible fiber-optic probe and a detection system consisting of a spectrometer and a CCD camera.

* Record spectra from the medically interesting tissue constitutes such as for instance cholesterol, NADH, elastin and collagen.

* Record spectra from different tissue types and try to identify differences and similarities.

* Theoretically "optimise" the set-up. That is, evaluate the different parts and estimate the improvements, performances and cost for a set-up consisting of optimised equipment.

3 Theory

3.1 Introduction

This chapter deals with the theoretical background to Raman spectroscopy. There are a number of books in this subject alone, and what is presented here is of course only a brief introduction to the physics involved in the technique. Nevertheless, the basic theory behind Raman scattering is fairly simple and the short section in this subject should be enough to give the reader a general understanding of the phenomenon.

Also, another light-matter interaction is discussed here, namely fluorescence. In biological materials fluorescence often is 10^6-10^8 times stronger than the Raman signal, and thus limits the possibilities to obtain a pure Raman spectrum. This puts high demands on the equipment used and methods to reduce the influence of fluorescence must be employed. In the last sections of the chapter the basic equipment for a Raman spectroscopy set-up is described and finally a set-up adapted to be more suitable for medical use is described.

3.2 Basic Theory of Raman Scattering

3.2.1 Quantum-Mechanical Approach

Quantum-mechanics provides an illustrative picture of Raman-scattering and is indispensable for a complete understanding of this phenomenon. (A brief introduction to the world of quantum-mechanics is given in appendix A and further reading is found in Refs [10,14]).

Consider two energy levels in an atom as illustrated in Fig. 3.1 (cf. Fig. A1 in appendix A) Normally one says that interaction between an atom and a photon is only allowed if the energy of the photon exactly corresponds to an energy gap between the levels (resonance). The photon may then momentarily excite the atom to the higher energy state and through immediate relaxation a new photon is created, scattered in an arbitrary direction.(Fig. 3.1a)

This is not completely true. Even if it is not resonance conditions, interaction can still occur in a two-photon scattering process. The incoming photon then excites the atom to a so called virtual level. Since this is no real, allowed, level relaxation immediately follows, resulting in a new scattered, photon. (Fig. 3.1b)

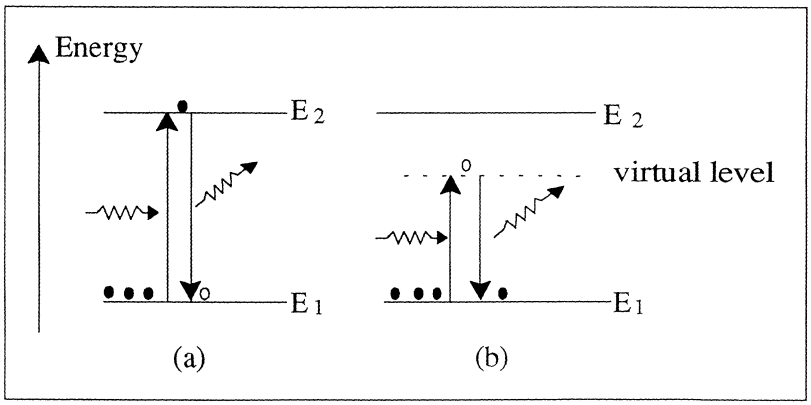

Fig. 3.1 Resonant and non-resonant scattering.

A more complex energy level scheme for a molecule (cf. Fig. A2 Appendix A) gives rise to several interesting alternatives for this process. (Fig. 3.2)

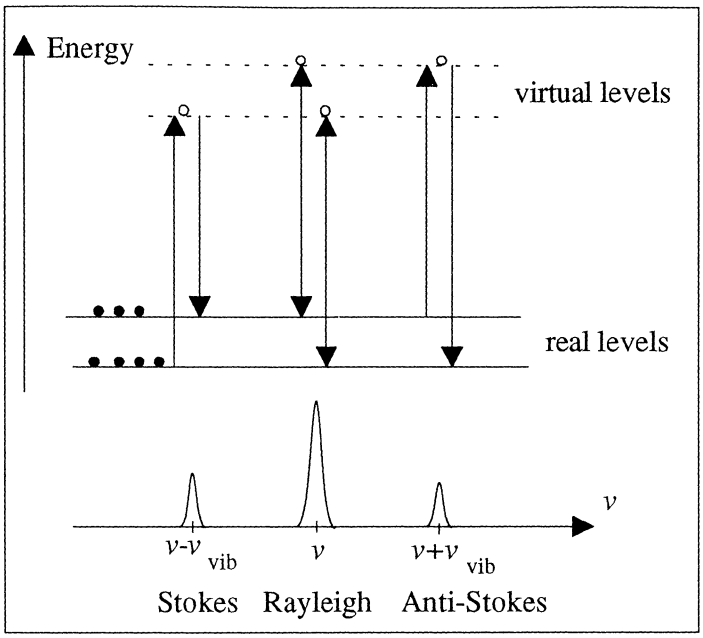

Fig. 3.2 Rayleigh- and Raman- Scattering

If the initial and final levels are the same, the incoming and the scattered photon will have the same energy and elastic so called Rayleigh scattering has occurred. Different initial and final levels lead to a lower (Stokes scattering) or even higher (Anti-Stokes scattering) energy for the scattered photon. Both these two inelastic scattering events to are called Raman scattering, after the Indian scientist C. V. Raman who discovered this phenomenon in 1926.

The energy shift of the incoming and scattered photon thus equals the level-splittings of the molecule.It is different vibration and rotation possibilities of the molecule that causes these level splittings (cf. appendix A). In the wavelength region used in this work, however, interaction primarily occurs with vibrational splittings. These can be written:

$$\Delta E = h \nu_{vib} \qquad (3.1)$$

Thus the frequency shift of the Raman signal is equal to ν_{vib}, which is the ground frequency of the involved vibration.

3.2.2 Classical Approach

To gain further understanding of these scattering-phenomena the quantum-mechanical explanation has to be complemented by a classical picture. In this approach the light is seen as an oscillating electric field:

$$E = E_0 \cos 2\pi\nu t \qquad (3.2)$$

The electrically charged particles in a molecule are affected by such an external field, causing a displacement from their average-positions. This displacement results in an induced dipole-moment P in the molecule:

$$P = \alpha E = \alpha E_0 \cos 2\pi\nu t \tag{3.3}$$

The polarisability α is basically a constant of proportionality. However, due to the frequent asymmetry of molecules, P is usually not directed along E. The polarisability then include a change of direction and α is said to be a polarisation-tensor.

In a vibrating molecule the different possibilities of movement (rocking, twisting in different bindings) are called vibrational modes. By describing the movement in the molecule as a harmonic oscillator, the displacements from the equilibrium configuration can be written:

$$Q = Q_0 \cos 2\pi\nu_{vib} t \tag{3.4}$$

Where ν_{vib} is the vibration frequency as mentioned above. As the molecule vibrates, the polarisability usually changes as the configuration of the molecule changes.
Thus the polarisability α is a function of the displacement Q. For small vibrations, which means small displacements, the polarisability can be expressed in a Taylor-series:

$$\alpha(Q) = \alpha_0 + \left(\frac{\partial\alpha}{\partial Q}\right)\cdot Q + \text{ (higher order terms)} \tag{3.5}$$

Inserting (3.4) and (3.5) in (3.3) the yields:

$$P = \alpha_0 E_0 \cos 2\pi\nu t + \left(\frac{\partial\alpha}{\partial Q}\right) Q_0 E_0 \cos 2\pi\nu t \cdot \cos 2\pi\nu_{vib} t \tag{3.6}$$

Which with of the trigonometric identity $\cos\varphi\cos\theta = \frac{1}{2}[\cos(\varphi+\theta)+\cos(\varphi-\theta)]$ can be written as:

$$P = \alpha_0 E_0 \cos 2\pi\nu t + \left(\frac{\partial\alpha}{\partial Q}\right)\frac{E_0 Q_0}{2}\left(\cos 2\pi(\nu+\nu_{vib})t + \cos 2\pi(\nu-\nu_{vib})t\right) \tag{3.7}$$

This describes an oscillating dipole, which, according to classical theory, emits an electric field with the frequencies ν and $\nu \pm \nu_{vib}$. This is in agreement with the quantum-mechanical result.

3.2.3 Raman-Activity and Scattering Intensity

The classical expression Eq. 3.6 describes several important properties of Raman-scattering. The first thing we notice is that an absolute demand for the scattering to occur at all is that $\frac{\partial \alpha}{\partial Q} \neq 0$, which means that the polarisability α must change when the displacement Q changes. Such a vibration-mode is said to be Raman-active. This means that some molecules show comparatively strong Raman-signal while others (like water) show none, or very weak Raman features. Raman active or not depends on, for instance, symmetry and type of binding involved. A further description of these matters is found in for instance Refs [13,16,17].

Raman spectroscopy thus maps the vibrational splittings in a molecule. These splittings (as well as the rest of the energy level scheme) are characteristic of the molecule, and hence the Raman spectrum is a finger print, suitable for identification of substances. The energy shift as well as the scattering intensity characterises the spectrum. A number of typical Raman spectrums are found in e.g. Ref [18].

For the intensity from an oscillating dipole classical theory yields:

$$I = \frac{2}{3c^3}\overline{\left(\frac{\partial^2 P}{\partial t^2}\right)^2} \tag{3.8}$$

Which in combination with (3.7) gives:

$$I_{Rayleigh} = K_R \nu^4 I_0 \alpha_0^2 \tag{3.9}$$

$$I_{Stokes} = K(\nu - \nu_{vib})^4 I_0 \left(\frac{\partial \alpha}{\partial Q}\right)^2 \tag{3.10}$$

$$I_{Anti-Stokes} = K(\nu + \nu_{vib})^4 I_0 \left(\frac{\partial \alpha}{\partial Q}\right)^2 \tag{3.11}$$

Here K and K_R are constants and I_0 is the intensity of the incident light. These equations show a very strong frequency-dependence in the scattering-intensities ($I_{scattered} \propto \upsilon^4$) and that the relation between the intensities is independent of incident intensity I_0. Unfortunately the classical view falsely predicts that the strength of the anti-Stokes component should only differ from the stokes component by the ratio $[(\nu - \nu_{vib})/(\nu + \nu_{vib})]^4$.
Experiments show a bigger difference in strength, which is easily justified with quantum-mechanical theory. As mentioned in the brief chapter in this matter (Appendix A) the natural state for an atom normally is the lowest possible from an energy point of view. Hence, many fewer atoms are found in the upper state leading to the anti-Stokes process. This consequently results in a weaker component compared to the Stokes-component.

The relation between the populations in two levels separated by the energy dE is described by the Boltzmann law:

$$N_{upper}/N_{lower} = \exp(dE/kT) \tag{3.12}$$

Where k is the Boltzmann constant and T the absolute temperature in Kelvin. By combining this expression with Eq. 3.4 and Eq. 3.5 we get:

$$\frac{I_{Stokes}}{I_{Anti-Stokes}} = \frac{(\nu - \nu_{vib})^4}{(\nu + \nu_{vib})^4}\exp(dE/kT) \tag{3.13}$$

For a normal splitting of 0.10 eV and 800 nm excitation light in room temperature this relation gives $I_{Anti-Stokes} \approx 0.01 I_{Stokes}$ for 800 nm excitation light. This is in agreement with experimental results and since the Anti-Stokes component is so weak, it is usually not used for practical applied spectroscopy.

The relation between the Rayleigh- and Raman-intensities also depends on α and $\partial\alpha/\partial Q$ which can be theoretically calculated, using more quantum mechanics. This will not be done here, but it leads to the following rule of thumb (Refs [10,12]): $I_{Raman} \approx 10^{-5} - 10^{-3} I_{Rayleigh} \approx 10^{-8} - 10^{-6} I_{Incident}$

More on atomic physics and quantum mechanics is found in Ref [14] and on electromagnetic fields in Ref [15]. Spectroscopy and a number of applications is described in for instance Ref [10], while Refs [12,13] deals more with Raman spectroscopy for medical use.

3.3 Fluorescence

Fluorescence occurs when the energy of the incoming photons exceeds the gap between the energy levels, or energy bands, in a molecule and is able to excite the molecule to the upper band. The electron then first radiationless relaxes down to the bottom of the upper band, and from there it falls back down to one of the states in the lower band, emitting light with an energy corresponding to the length of the fall. (cf. Fig. 3.3)

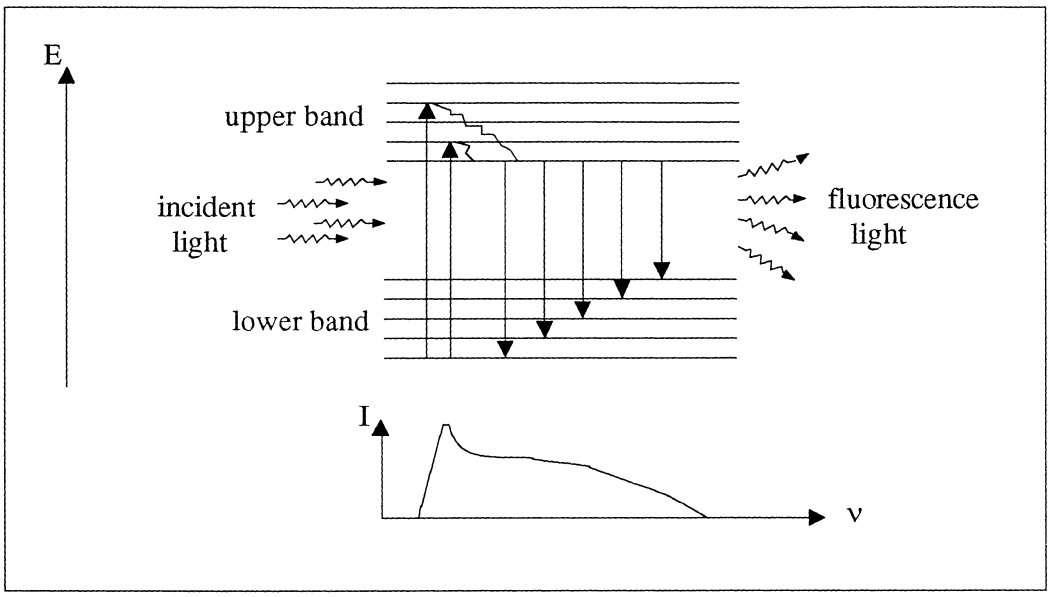

Fig. 3.3 Fluorescence

Obviously this light also contains information of the investigated sample, but usually this broadband emission is rather featureless and contains less information than a Raman-spectrum. In some cases, however, for instance in combination with a tumour-seeking agent with a characteristic fluorescence signature, fluorescence spectroscopy is an excellent diagnostic method. (Refs [10,19,20])

For Raman spectroscopy there are several techniques to surpress the influence of fluorescence. By using excitation light with low energy photons (long wavelength), agents to decrease the fluorescence or clever analysis methods the influence of fluorescence is reduced in the results.

3.4 Conventional Set-Up for Raman Spectroscopy

In theory and for qualitative studies, the set-up for Raman spectroscopy is fairly simple. In their first experiments Raman and Krishnan used the sun as a light-source and visually detected the frequency shift as colour-changes in the scattered light.

Naturally, modern scientific applications of Raman-spectroscopy use more advanced techniques, but the principle of the set-up is still very much the same, although the performance of the equipment has improved dramatically. Basically, the scattered light from a monochromatic light source is analysed in a wavelength-dispersive collection and detection system.

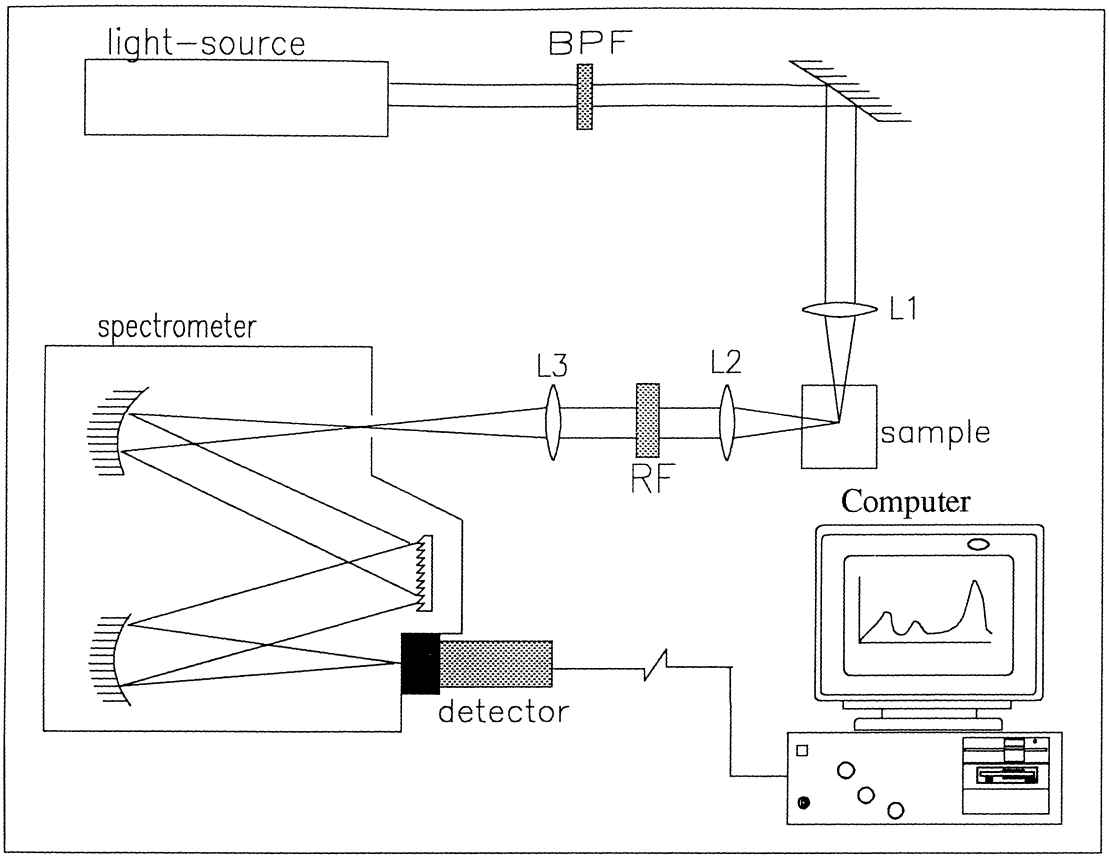

Fig. 3.4 Conventional Raman spectroscopy set-up, BPF-Bandpassfilter, RF-Ramanfilter, L-lens

The light source. As light source producing the incident photons in a modern Raman spectroscopy set-up, lasers are the only ones really worth considering. For Raman spectroscopy lasers show outstanding performance compared to conventional light sources offering monochromatic light at high intensities in a variety of wavelengths.

Filters and optics. Although the laser is a great monochromatic light source it is not perfect and often a bandpass-filter (BPF) has to be introduced in the beam-path to get rid of any weak emission outside the actual laser line. If not properly filtered, this emission result in unwanted artificial peaks in the weak Raman-spectrum.

Usually the excitation light is focused onto the sample with a focusing-lens (L1). The focusing is not essential, but it makes the collection of the scattered light simpler, since it is easier to collect light from a small intense spot than from a weaker wide source.

The scattered light is collected and focused into the spectrometer by two other lenses (L2,L3) and usually also filtered through a so called Raman-filter (RF). The function of this filter is to suppress the strong Rayleigh-component and thereby simplify the analysis of scattered light. This component otherwise causes difficulties for instance by being rediffracted and reflected in the spectrometer and influence and obscure the Raman spectrum.

The spectrometer. Before reaching the detection system, the collected light is separated in its different wavelength-components in a spectrometer. Most Raman spectrometers use one, two or even three gratings to disperse the light. Each grating increases the resolution and the efficiency of separating the strong Rayleigh-light from

the weak Raman signal. The disadvantage of using several gratings is decreased transmission of the spectrometer, which further decreases the already weak Raman signal.

The detection system. The spectrum can be analysed either by a single channel (scanning) or a multi channel detection system. In a single channel system the intensity of one wavelength component is measured at the time for instance with a photomultiplier-tube. The grating in the spectrometer is then slowly turned to scan the spectrum over the detector. This method is cheap, simple and sensitive, however not light economic.

Alternatively, all the wavelength components are registered simultaneously by several hundreds of small detectors in a multichannel system. The advantage is of course that the whole spectrum is recorded at the same time, which not only gives a shorter integration time, but also the possibility to follow dynamic events.

3.5 Medical Adaption of the Set-Up

As the goal is to perform *in vivo* medical measurements, one important limitation obviously is the short acquisition times possible. Other important features, critical for a system for medical use are reliability, flexibility, as well as economical aspects. Hence, in the choice of equipment for the set-up to be developed, one has to meet several different demands. This will lead to a row of compromises, each with its advantages and drawbacks.

The first compromise is the choice of wavelength. Both the fluorescence and the Raman signal decrease with an increased excitation wavelength (cf. chapter 3.2.3 and 3.3). This gives two alternatives: Either a short excitation wavelength can be used which indeed gives increased fluorescence but an even higher increase in the intensity of the Raman scattering (cf. Eq. 3.9 and Eq. 3.11). For medical use, however, this alternative is unfavourable since short wavelength radiation causes several hazards to the living cells.

In the second alternative, a longer wavelength is chosen where the fluorescence is reduced but an acceptable Raman signal still is obtained. This means a near infra-red wavelength in the 800 nm region.

As a light source in this wavelength region a diode-laser is very favourable. It is cheap, reliable and easy to handle, but unfortunately comparatively weak. (The light intensity at the tissue is of course limited anyway, due to medical reasons) The single element diode-lasers needed for Raman spectroscopy are today not able to produce as high output-powers as could be medically acceptable. However, limits (medical or practical) in the light intensity at the sample leads to a weak signal, resulting in increased demands of efficiency and sensitivity in collection- and detection-system

Basing the set-up on optical fibre delivery offers flexibility by a convenient way of leading the excitation-light to the sample, although on the expense of some light losses. Furthermore, an optic fibre also works excellent as collection optics, collecting and leading the scattered light to the detection system. Excitation and collection fibres can be combined in a single probe.

As the Raman signals are weak, high transmission of the Rayleigh-rejection filter and the spectrometer are required. Holographic filters are the best rejection-filters available

today. They transmit up to 90% of the light outside a very narrow (FWHM around 20nm) rejection interval and efficiently surpress the Rayleigh-scattered light by a factor of up to 10^6. This allows recording of weak Raman-signals close to the laser line.

The throughput of the spectrometer depends essentially on the number of gratings and the f-number of the optics (f/# is focal length through by optically usable diameter). A single grating and a low f/# give the highest throughput. The spectral resolution needed in the recordings sets the limit of the throughput.

A multichannel detection system is the fastest and the most preferable detector is then a CCD-camera. Unfortunately the CCD-chip quickly looses it sensitivity as we move up in the infrared region.

Further discussions in the choice of equipment are found in chapter 7.

4 Atherosclerosis-a Medical Introduction

4.1 Introduction

The aim of this chapter is to give an introduction to the medical background of the vascular disorder atherosclerosis. Therefore, the structure of blood vessels is briefly described as well as the origin and development of atherosclerotic plaque. Its major complications, including myocardial infarction and ischemic heart disease, causes more than 50% of the annual morbidity in the United States (Ref [21]). Consequently much effort and money have been put down to understand and cure this serious disorder. Despite intense research the reasons for the disorder are not completely understood, although its development and consequences are well investigated.

Atherosclerosis affects the arteries, causing a raised focal plaque which compromises the blood flow and causes thrombosis and hemorrhage. The plaque consists of a core of accumulated lipids (mainly cholesterol and cholesterol esters), covered by a fibrous cap. The aorta and the coronary and cerebral systems are most commonly affected, resulting in aortic aneurysms and myocardial and cerebral infarction as the major consequences.

Several risk factors are identified and extensively investigated in the development of atherosclerosis:

* Atherosclerotic plaque is rich in **lipids** (cholesterols, etc.) derived from the blood. Abnormal amounts of these substances caused by for instance fatty diets or genetic disorder increases the risk of developing serious atherosclerotic plaque.

* There is also a clear, although not completely understood, connection between high blood pressure -**Hypertension**- and atherosclerosis.

* Atherosclerosis among **smokers** is more extensive and severe than among non-smokers. Thus the incidence of myocardial infarction and aortic aneurysms is increased among smokers.

* **Diabetics** are more commonly affected by atherosclerosis and most other occlusive vascular disorders.

Other risk factors, often referred to as soft, since they are difficult to clinically verify, are insufficient physical activity, stressful lifestyle and obesity.

Everybody develops atherosclerosis to some extent, but summary of the risk-factors puts men in the western world and at increasing age in the highest risk-group. Interesting is also the remarkably low rates of death related to atherosclerosis found in for instance Japan compared to the US. Migrated Japanese, however, who adopts the American lifestyle and dietary customs, show the same risk for developing the disorder as the rest of the American population (Ref. [21]), which confirms the view on atherosclerosis as a welfare-disease.

Atherosclerotic plaque causes several hazards to the vascular system. The following have the most clinical significance:

* Naturally atherosclerosis causes **reduction of blood flow** and thereby ischemic diseases and gangrene of extremities.

* **Hemorrhage** either in the fibrous cap or inside the plaque which may induce rupture.

* **Rupture** or **ulceration** of the luminal surface of the atherosclerotic plaque may release thrombogenic substances into the vessel. This may cause **thrombosis**, the most feared complication, which partly or completely occlude the lumen.

* Almost always the affected arteries undergo **calcification**, resulting in eggshell brittleness of for instance the aorta.

4.2 Blood vessels

The vessel-walls in the elastic and muscular arteries, mainly affected by atherosclerosis, consists of three layers -or tunicas - intima, media and adventia.

The intima is composed of a lining of endothelial cells and a thin layer of connective tissue. The endothelial cells are responsible for the interaction between blood and tissue by controlling the transfer of molecules and blood components in both directions. Thus the function of the endothelium is both important and complex and not surprisingly atherosclerosis and several other arterial diseases are caused by dysfunction or injury in the endothelium.

Separating the intima and media is an internal elastic lamina through which smooth muscle cells (SMC's) can migrate from the media to the intima. The media consists mainly of these SMC's circularly or spirally arranged to regulate local blood flow through contraction and relaxation. In the largest arteries (including the aorta) elastic fibers are interposed between the SMC's, allowing the vessel to expand and recoil to minimize energy-losses due to the pressure changes between diastole and systole.

The outermost layer, the adventia, is separated from the media by an external elastic lamina and mainly consists of connective tissue, small vessels and nerves.

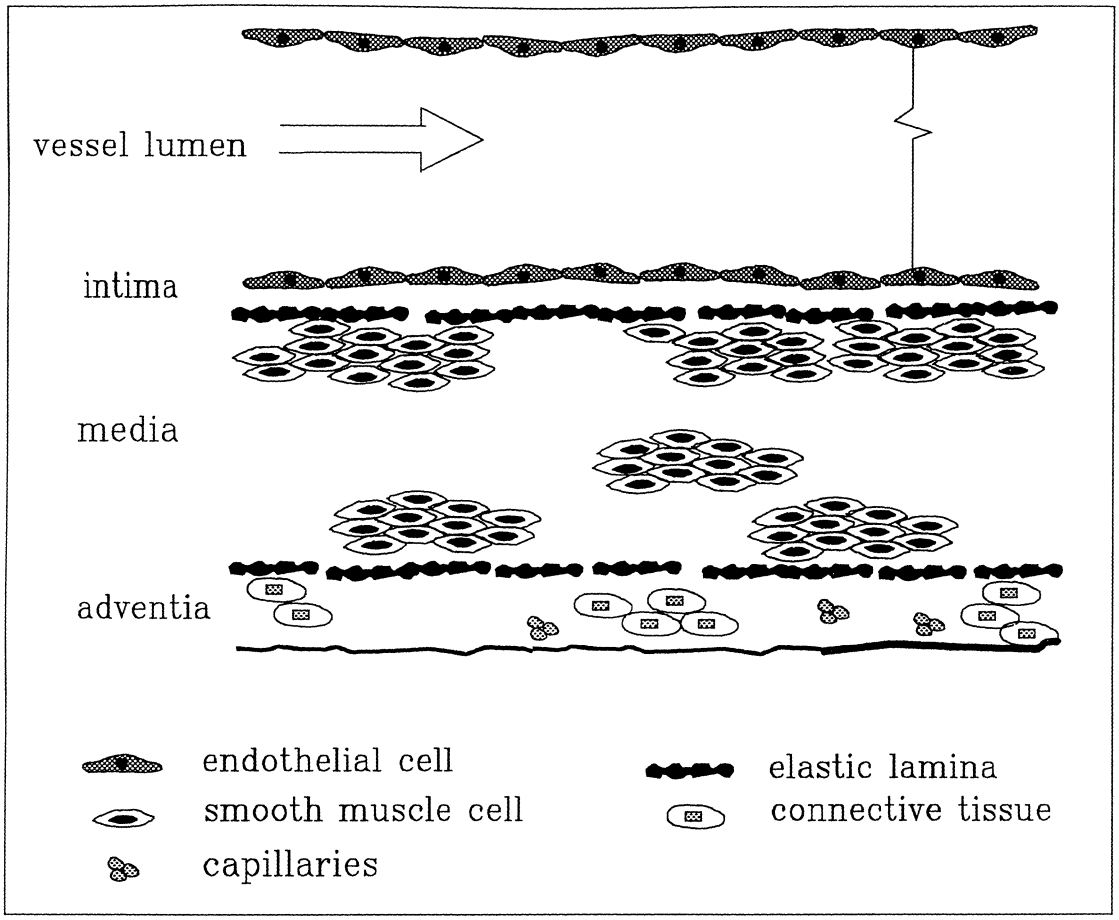

Fig. 4.1 Schematic drawing of a blood vessel (not in scale)

4.3 Atherosclerosis

Although not explaining all aspects of, and reasons for, atherosclerosis the *response to injury hypothesis* gives a good picture of the development of the disorder. (Refs [21,23]) An injury to the endothelium or dysfunction in this lamina increases the permeability for blood components. This causes blood monocytes and platelets to adhere to the endothelium and monocytes enter the intima, where they transform into macrophages. Macrophages proliferate in the intima but more important they ingest lipids (such as cholesterol) to produce foam cells. Platelets and macrophages release growth-factors stimulating SMC's to migrate from the media to the intima and proliferate. Furthermore SMC's also can accumulate large amounts of cholesterol and cholesterol esters and produce foam cells.

These effects can also be observed as a result of a physical injury to the endothelium and is a natural response- and protection mechanism from the body. In this case, however, it appears both uncaused and exaggerated.

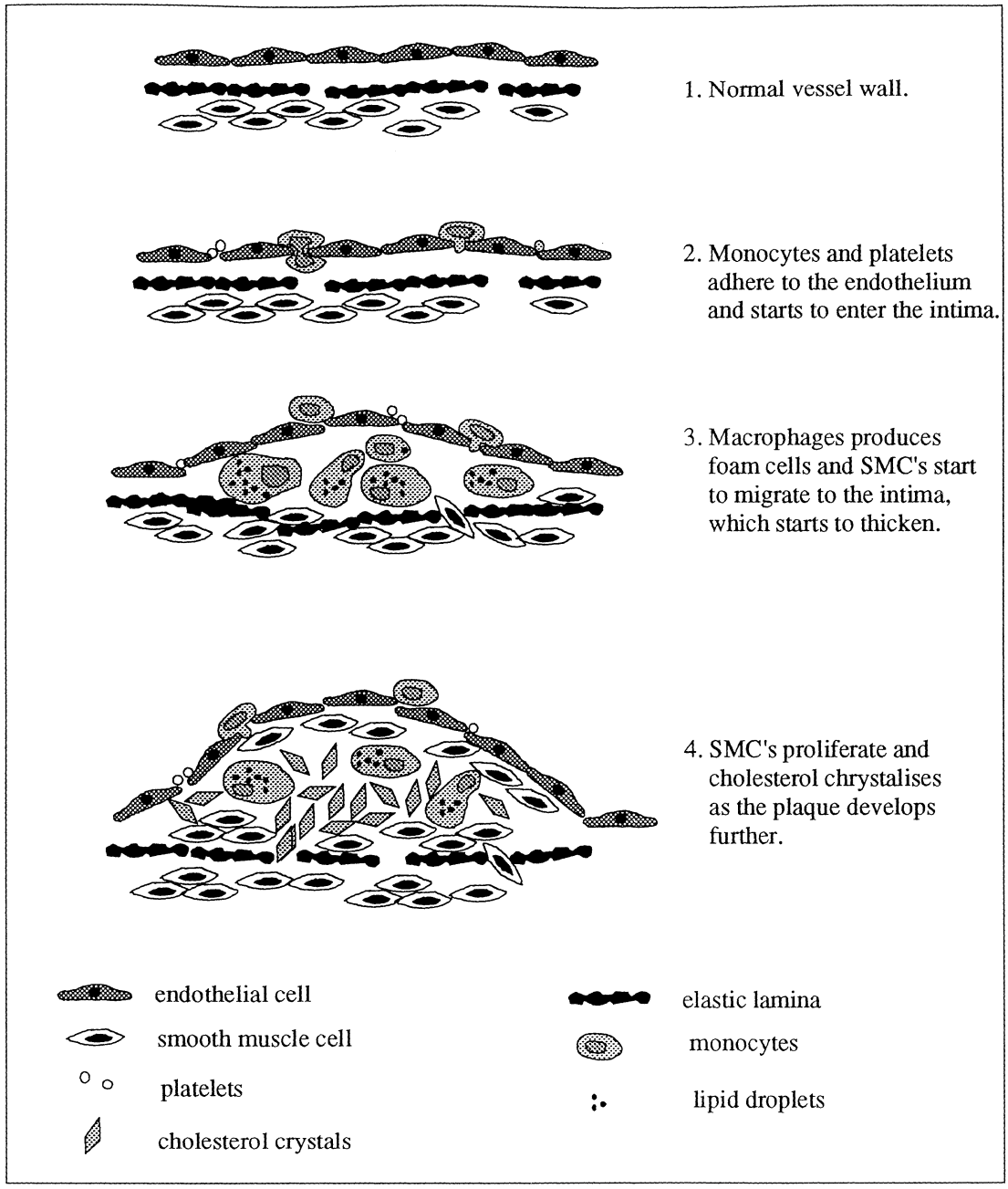

Fig. 4.2 Development of an atherosclerotic plaque. (from Ref. [21]) (not in scale)

Proliferating SMC's and macrophages together with production of foam cells results in a thickening of the intima and a narrowing of the vessel. Notable here is that the resistance to the blood flow is proportional to the fourth power of the diameter (i.e. halving the diameter increases the resistance 16-fold (Ref [22])) and therefore even a minor narrowing of the vessel strongly increases the resistance and decreases the blood flow.

As the disorder develops further, SMC's die from poor nutrition and develop into a necrotic core which also contains lipid-filled macrophages and cholesterol crystals. The core is covered by a fibrous cap of SMC's and macrophages.

Atherosclerosis developed this far seriously occludes the lumen and can easily rupture the vessel or cause thrombosis. If this happens in the heart or in the brain, the effects might be lethal.

A much more complete description of these medical matters are found in Refs [21,22,23].

4.4 Biochemistry

We will now try to identify the most significant biochemical changes caused by the development of atherosclerosis as these changes form the base for Raman spectroscopy with the aim to identify atherosclerotic lesions.

The first thing that happens according to the response to injury hypothesis is that the amount of smooth muscle cells in the vessel wall increases. This means a higher concentration of the macro-proteins *collagen* and *elastin* which are two of the main constitutes of muscular cells. (Ref [24])

Secondly, lipids are disposed in the vessel wall and foam cells are produced. The accumulated lipids are mainly *cholesterol* ($C_{27}H_{46}OH$) and cholesterol esters and as the disorder develops further they crystallize into *cholesterol crystals*.

Thirdly, in the final stages of serious plaque heavy calcification takes place and *hydroxyapatite* is formed. Hydroxyapatite is an interesting substance since it has a comparatively strong, characteristic Raman signal. On the other hand, it would be preferable to detect the disorder before it develops this far.

Further reading on biomedical changes and its spectroscopic consequences is found in Refs [1,2,22,24]

5 Experiments

5.1 Introduction

The conclusion of the theory chapter was that Raman-scattering is an inelastic process. This means that the frequency of the scattered light differs from the incoming, a frequency shift that was shown to correspond to the vibrational splitting between the energy-levels in the molecules.

These splittings are very characteristic for a molecule and the Raman spectrum is therefore a detailed fingerprint of the molecule, making the method suitable for medical (or chemical) analysis. Other key-features for medical applications are that Raman-activity of water and glass are weak, resulting in only weak signals from glass in optical equipment and water, always present in large quantities in tissue.

A major disadvantage, is as mentioned, the influence of fluorescence, which indeed has limited the development of analysis methods based on Raman-scattering, especially for biomedical applications.

In the previous chapter, we learned a little bit about blood vessels and the development and consequences of atherosclerosis. In the last section of that chapter the main constitutes of human tissue were discussed in order to get an idea of what to expect from Raman spectra of tissue samples.

In this chapter we will describe the samples and the set-up used for the measurements as well as which experiments that were carried out and why. We will also discuss the analysis method used to reduce the problem with strong fluorescence.

5.2 The Set-up

The principles of a set-up for Raman spectroscopy are described previously and the experimental arrangement used in this work is shown in Fig. 5.1. A short description of the individual parts is given below, and as mentioned earlier, the aim in choice of equipment is to get closer to a clinically usable set-up.

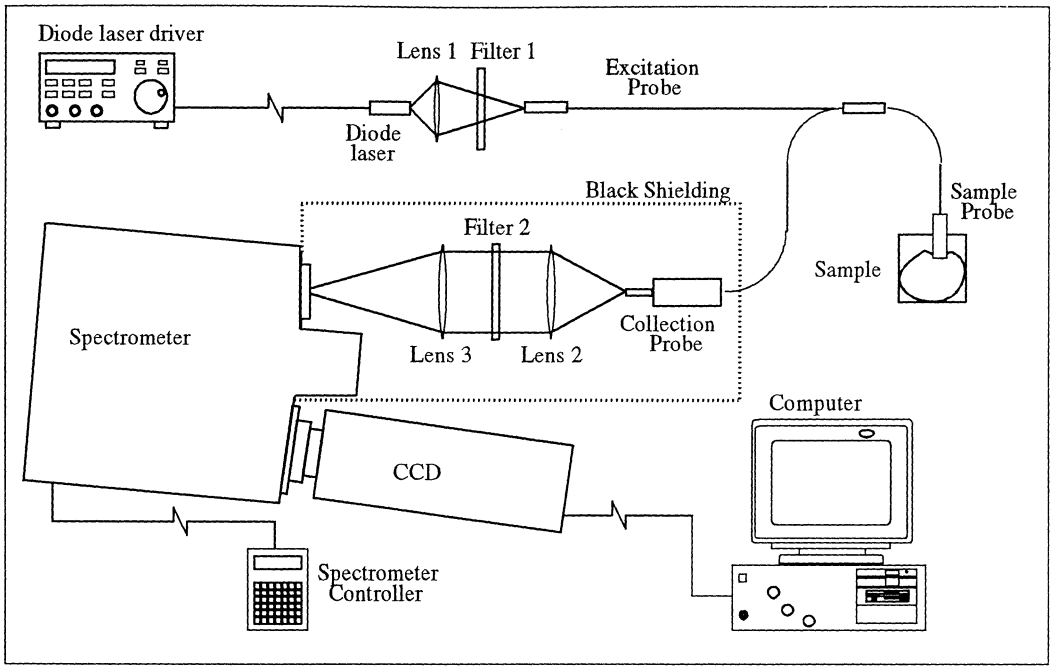

Fig. 5.1 The set-up

The excitation light source was a diode laser driven by a Melles Griot diode laser driver (06DLD203). The temperature of the laser diode was controlled from the same driver by use of thermoelectric cooling. Since output power and wavelength from diode lasers change with temperature, mode hops, wavelength drift and power changes otherwise would occur.

Two different lasers were used: One Sony laser (SDL 201-V3) producing 35mW of output light around 783nm and one Sharp (LTO24MDO) producing 20mW around 780nm. Of this light approximately 7mW reached the sample. The losses occurred in the coupling to the excitation fibres, which due to the poor spatial quality of the diode laser beams was comparatively inefficient, and in the bandpass filter

Filters and optics: The light from the laser was collected and focused on the excitation fibres with a lens (Lens 1: Melles Griot 06GLC002) mounted directly on the diode laser holder. In order to reduce the broad emission at the foot of the laser line a dielectric bandpass filter was placed between the lens and probe.

Light was guided to and from the sample by a fibre-optic probe (SFA 371-541L-1-01 from C-technologies) consisting of 37 excitation- and 54 collection fibres, all 100μm in diameter. The excitation fibres were circularly arranged in both ends. In the probe head, they were surrounded by the collection fibres, which in the collection end was arranged in a linear array, well matching the entrance slit of the spectrometer.

The collection optics consisted of a collimating lens (Lens 2), a filter and a focusing lens (Lens 3). Lens 2 was aimed to collect and collimate the light from the probe in order to get a parallel passage through the filter. The holographic notch-plus filter (HNPF-795-1.0) from Kaiser Optics was used to suppress the Rayleigh-scattered light, and since the attenuation wavelength of such a filter is dependent of the incident angle the light should be as parallel as possible. The last lens (Lens 3) focused the collected light onto the entrance slit of the spectrometer.

The Spectrometer: The light was dispersed by a Spex 270M single grating spectrometer (focal length 0.27m, f/4) remotely controlled by a Hand Scan hand held controller. The entrance slit was 1.5cm high and the width could be set between 0μm and 7000μm in steps of 6.25μm. Two different gratings were used in the spectrometer (grating 1: 1200g/mm, blazed at 750nm, dispersion: 3.1nm/mm and grating 2: 150g/mm, blazed at 500nm, dispersion: 24.8nm/mm)

The detector system was based on a liquid nitrogen cooled CCD-detector (Thomson CSF THX-31159 A) and an optical multichannel analyser (OMA4000) from EG&G Princeton. The system was used at a CCD-chip temperature of -120°C. According to the manufacturer the dark current at this temperature should be less than ten counts per pixel and hour. The CCD-array consisted of 512×512 charge-coupled pixels which, with each column electronically summed before readout, formed a 512-channel detector. Since the array was 9.7mm×9.7mm, and the pixels 19μm×19μm, each channel were 19μm wide and 9.7mm high.

The dispersions 3.1nm/mm and 24.8 nm/mm then results in a spectral coverage of about 30nm for the 1200g/mm grating and 240nm for the 150g/mm grating, or calculated from a 780nm laser-line, 470cm^{-1} and 3000cm^{-1} respectively.

5.3 Data Analysis

There are several different ways of reducing the influence of the strong fluorescence in Raman spectra from biological materials. As discussed in the theory chapter the first and most important thing is to choose the optimal wavelength in order to reduce fluorescence and still obtain a detectable Raman signal.

Secondly, different analysis methods can be used to subtract or filter out fluorescence in the recorded spectrum. Fourier transform filtering and other mathematical methods synthetically remove the fluorescence background. Usually these methods utilise the different nature of the broad-banded fluorescence compared to the sharper Raman-peaks.

In this work, however, a semi-mathematical shifted-wavelength-technique was used. The basis for this technique is the difference in the scattering processes of Raman scattering and fluorescence, meaning that a slight shift in the excitation wavelength will shift the Raman-peaks equally much, while the fluorescence remains fairly constant. In order to get rid of the fluorescence in the spectra from biological samples, two spectra were recorded

with different excitation wavelengths. Then one was subtracted from the other and the resulting differential-spectra was finally integrated to obtain a fluorescence-free Raman spectra. To compensate for small changes in the laser power between the recordings the spectra were calibrated to a common area before subtraction. The fact that the Raman signals are so much weaker than both the unshifted, scattered, excitation light and the fluorescence caused, due to imperfections in the recordings, some practical difficulties in this process.

Although a band-pass filter was used, there still remained a major base on the laser line. This resulted in a slope in the collected Raman-spectra. (cf. Fig. 6.1) Obviously this slope moves as the wavelength is shifted for the second recording and hence we are not only integrating the shift of the Raman peaks but also the change in the slope. To reduce the influence of this problem, the spectra were fitted to a second degree polynomial. This polynomial was subtracted from the raw spectra before further processing to produce a stable base-line.

A small matlab program took care of these mathematically simple steps and the matlab files are enclosed in Appendix B.

5.4 The Samples

The first measurements were made on liquid chemicals with characteristic strong Raman-spectra. These recordings were performed to get to know the equipment and to try out the performance of the set-up.

Secondly, spectra of pure tissue constitutes were recorded. The following samples were delivered by Sigma Chemical Company (P.O. Box 14508, St. Louis, MO 63178, USA):
Cholesterol ($C_{27}H_{46}O$), product number C8667.
NADH ($C_{21}H_{27}N_7O_{14}P_2Na_2$), product number N6005.
Collagen, product number C9879.
Elastin, product number E1625.
These substances are interesting since the abundance of these tissue-constitutes is likely to change as medical disorders such as atherosclerosis develops.

The third group of samples were tissue samples from a pig-heart. Unfortunately, no pathological human tissue-samples were available, which of course would have been even more interesting. Nevertheless, the different tissue types from the pig should not differ very much from human tissue, although pigs, unfortunately for this project, show no signs of atherosclerosis in their short life.

6 Results

6.1 Introduction

In most of the experiments performed, the 1200 g/mm grating was used, in order to obtain a sufficiently good spectral resolution. This grating of course gives a limited spectral coverage and therefore these spectra are put together from four individually recorded spectra. Some measurements on liquid chemicals, however, were made with the 150 g/mm grating and which grating that was used in each case is indicated together with the integration time at each presented spectrum.

All spectra were recorded with a 50 μm slit width and with integration times ranging from 0.1 s up to 500 s. The spectra were background subtracted but not compensated for the wavelength dependence of the filters and detector.

6.2 Liquid Chemicals

As mentioned earlier these measurements were performed mainly to test the equipment and try out the performance of the set-up. Therefore only the spectra from nitrobenzol are presented here. All these spectra were recorded with the Sharp laser running at 779.1 nm.

Fig. 6.1 shows a broad spectral region covering both laser line and Raman spectra. The 150 g/mm grating was used and the integration time was 30 s.

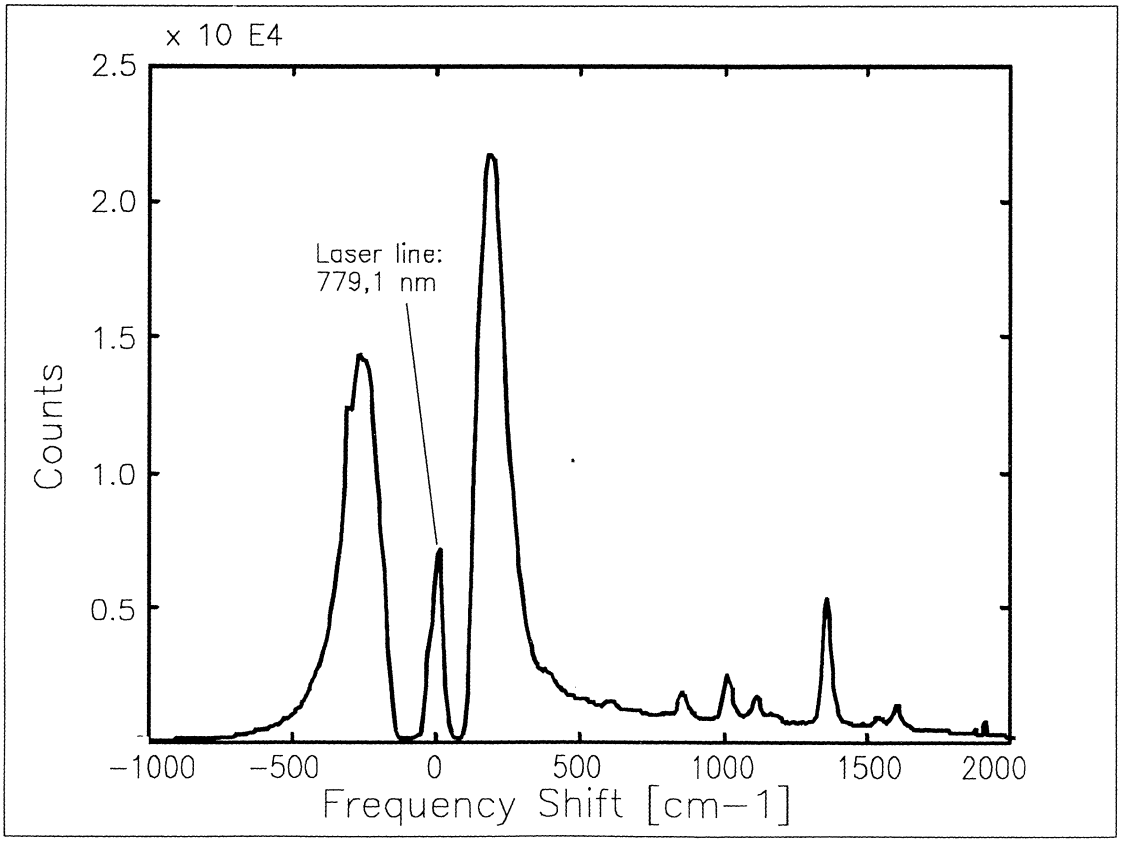

Fig. 6.1. Raman spectra of Nitrobenzol (150 g/mm grating and 30 s integration time)

The strongly suppressed laser line is seen at 0 cm^{-1} (779.1 nm) and despite the bandpass filter there still remains a major base on the laser line resulting in a slope in the Raman spectrum. The major Raman peaks from nitrobenzol are observed between 600 cm^{-1} and 1600 cm^{-1} and this spectral region is also shown in Fig. 6.2.

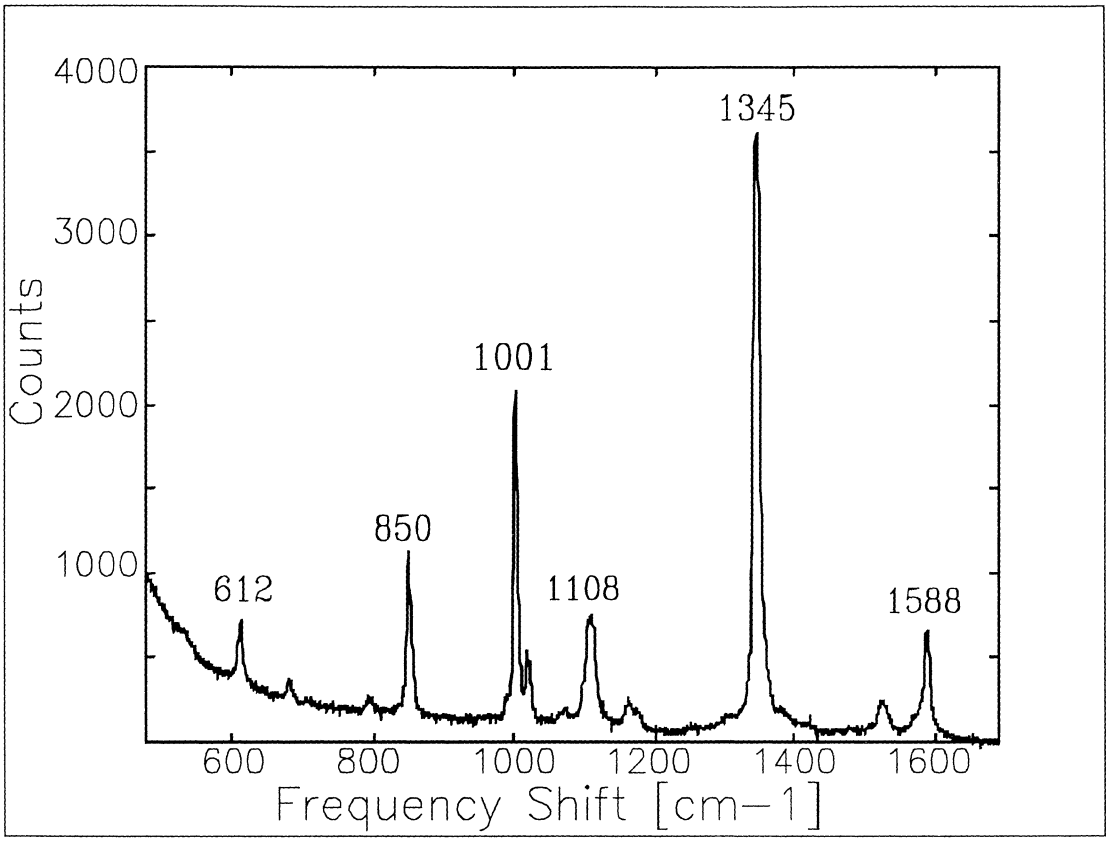

Fig.6.2. Raman spectra of Nitrobenzol (1200 g/mm grating and 30s integration time)

The spectrum in Fig.6.2 is recorded with the 1200 g/mm grating and the higher resolution reveals more details in the spectrum. The energy shifts of the major peaks are also indicated in the figure and the results are in good agreement with other literature values such as these in Ref [13] and Ref [18].

In Fig. 6.3 four spectra, recorded with different integration times, are presented. To decrease the influence of high-frequency noise, these spectra were smoothened using an average filter five pixels wide. Naturally the quality of the Raman spectra gradually decreases as the integration time gets shorter, but the major peaks are distinguishable all the way down to an integration time of 0.1 s.

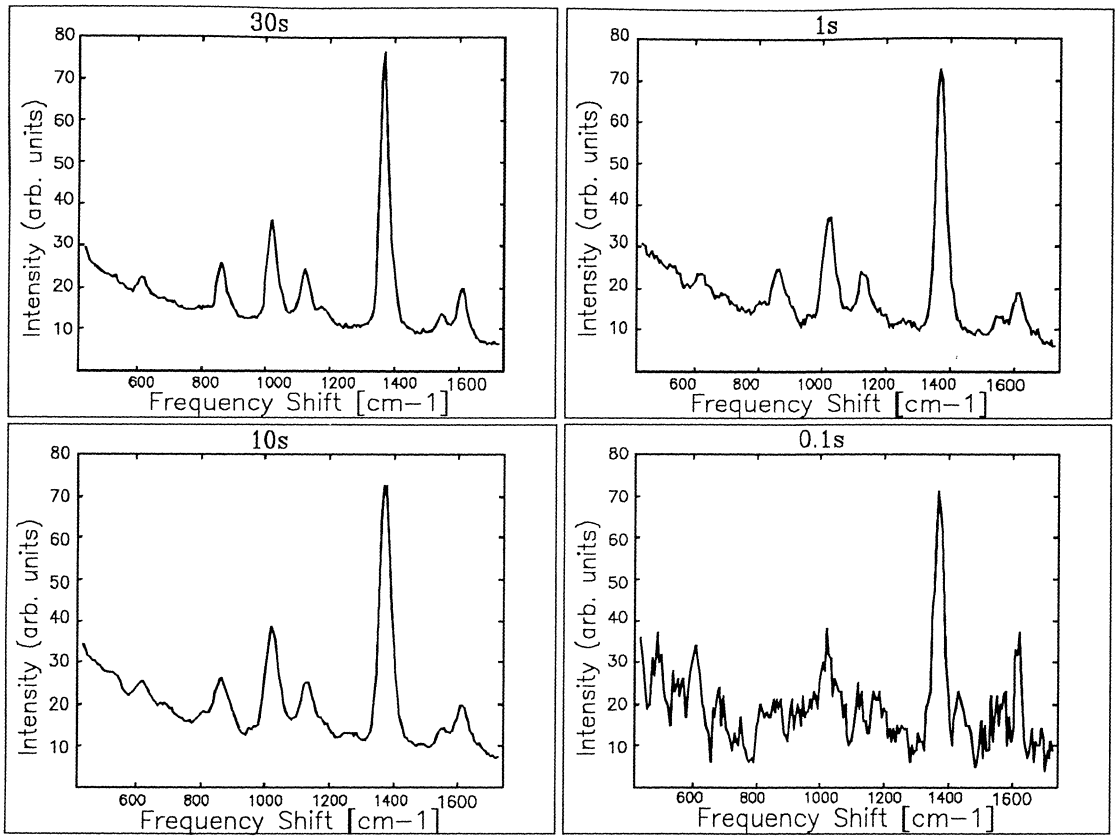

Fig.6.3. Raman spectra of Nitrobenzol (150 g/mm grating and 30-0.1 s integration time)

6.3 Pure Tissue Constitutes

All spectra from tissue constitutes were recorded with the 1200 g/mm grating and because of the strong fluorescence from these materials the shifted wavelength technique was used. The Sharp laser (779.1 nm and 781.7 nm) was used for the measurements on cholesterol and NADH. The recorded spectra are shown in Figs. 6.4 and 6.5.

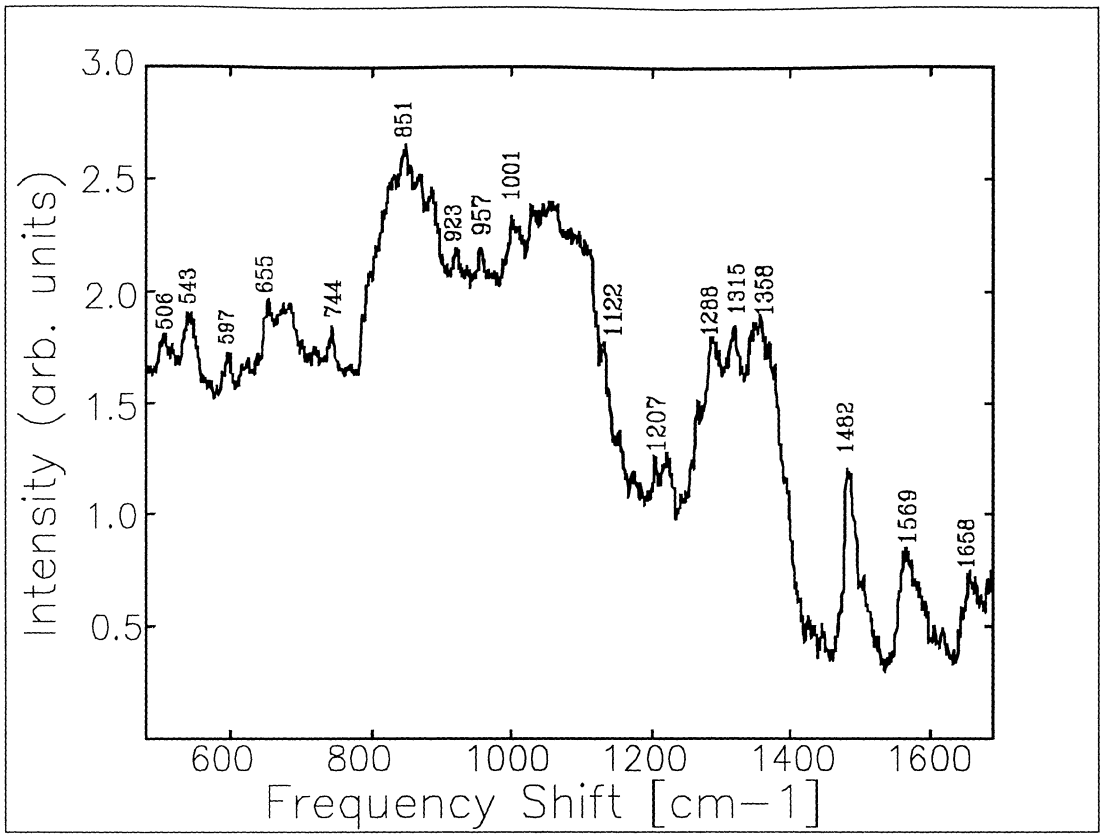

Fig.6.4. Raman spectra of Cholesterol (1200 g/mm grating and 200 s integration time)

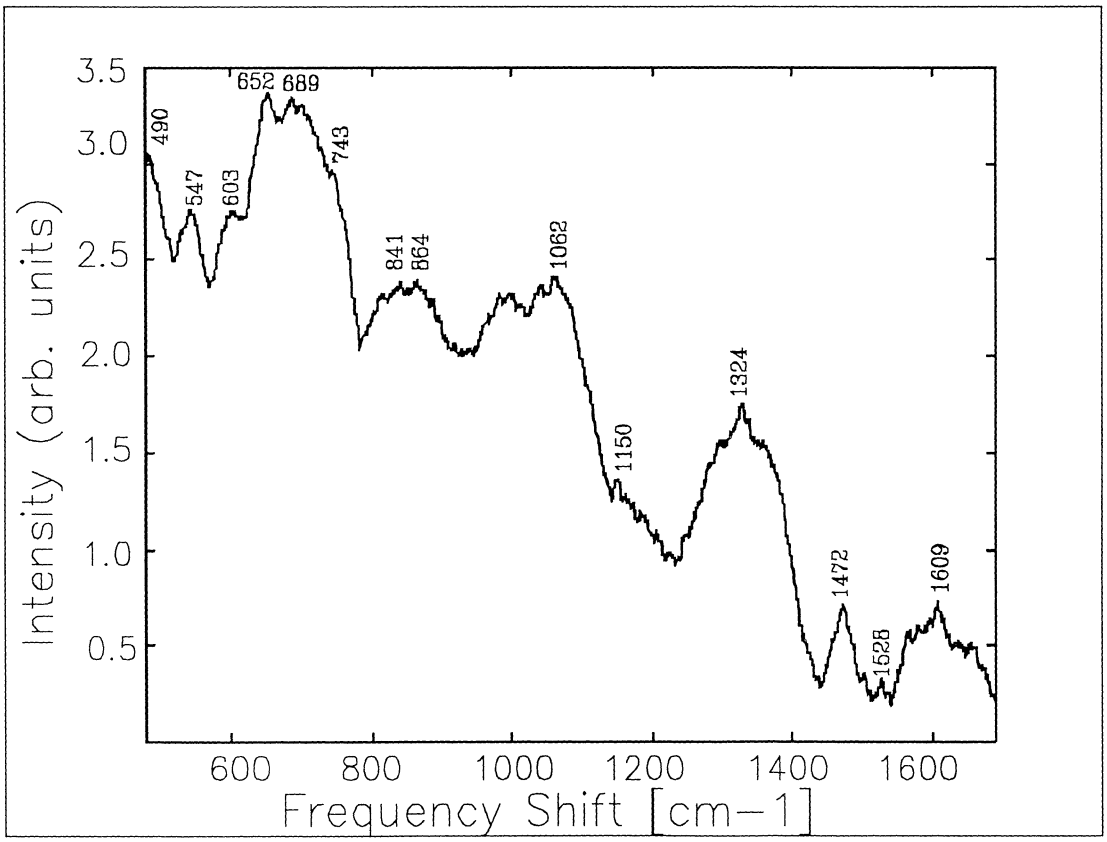

Fig.6.5. Raman spectra of NADH (1200 g/mm grating and 200 s integration time)

The fluorescence and the laser line base interfere rather badly in these spectra resulting in a varying background. Still a number of Raman peaks can be identified. The spectra from cholesterol and NADH can be compared for instance with the results of Carlsson and Bood (Ref [13]) or Faiman (Ref [24]) (cf. Appendix C).

Some peaks (e.g. 543, 597, 851, 957 cm^{-1} for Cholesterol and 1062 cm^{-1} for NADH) show good agreement while some others (e.g. 700, 1482, 1569 cm^{-1} for Cholesterol and 547, 1472 cm^{-1} for NADH) are either very faint or seem to be displaced.

The spectra from Elastin and Collagen shown in Fig. 6.6 and Fig. 6.7 were recorded with the same integration time and wavelengths

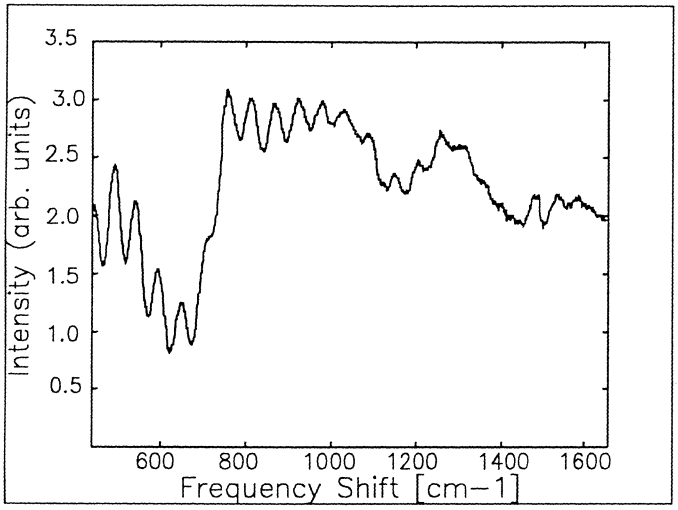

Fig.6.6. Raman spectra of Elastin
(1200 g/mm grating and 200 s integration time)

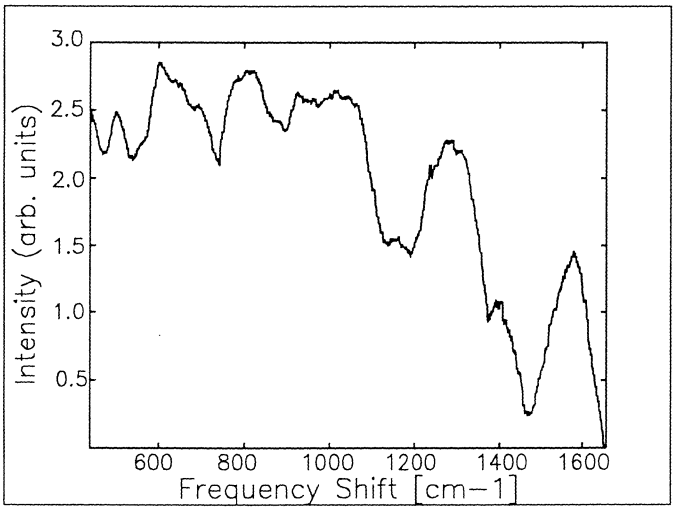

Fig.6.7. Raman spectra of Collagen
(1200 g/mm grating and 200 s integration time)

These spectra are even worse influenced by strong fluorescent and few, if any, Raman peaks can be distinguished. The oscillating pattern in the left half of Fig. 6.6 is probably a result of change in the laser-line slope as the wavelength is shifted and could not be regarded as Raman peaks.

6.4 Tissue from Pig-Heart

Spectra from four different tissue types were recorded and the results are presented in Figs. 6.8-6.11. These spectra were recorded with the Sony laser (782.2 nm and 784.0 nm) and 500 s integration time.

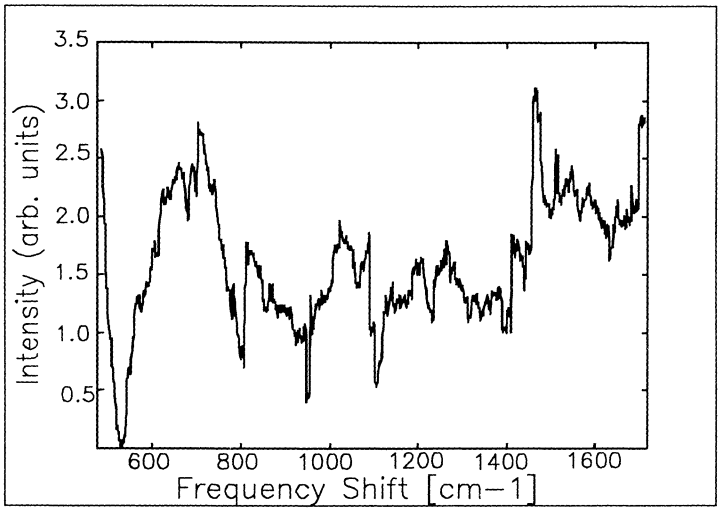

Fig. 6.8. Raman spectra of a Heart muscle
(1200 g/mm grating and 500 s integration time)

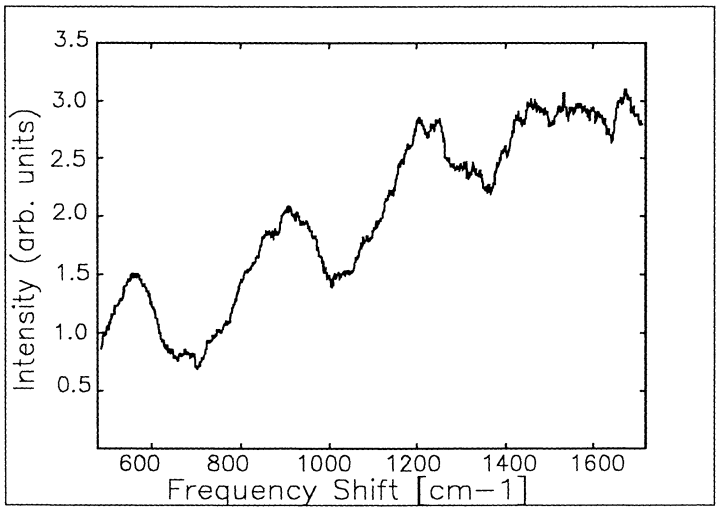

Fig. 6.9. Raman spectra of an Aorta
(1200 g/mm grating and 500 s integration time)

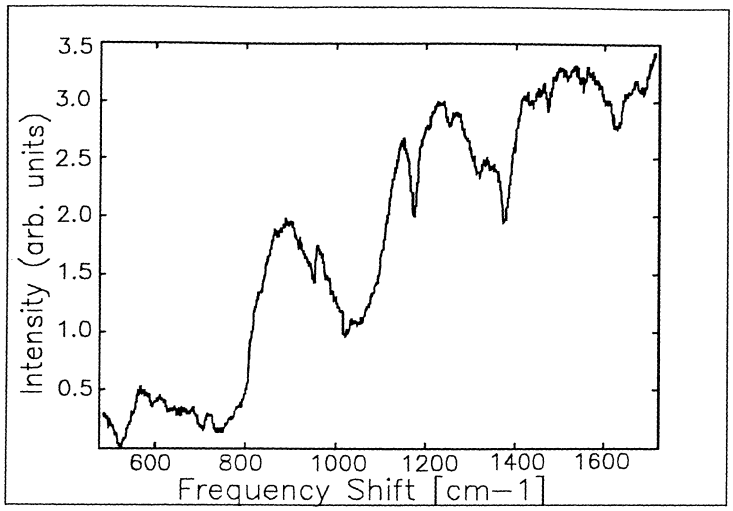

Fig. 6.10. Raman spectra of a Vein
(1200 g/mm grating and 500 s integration time)

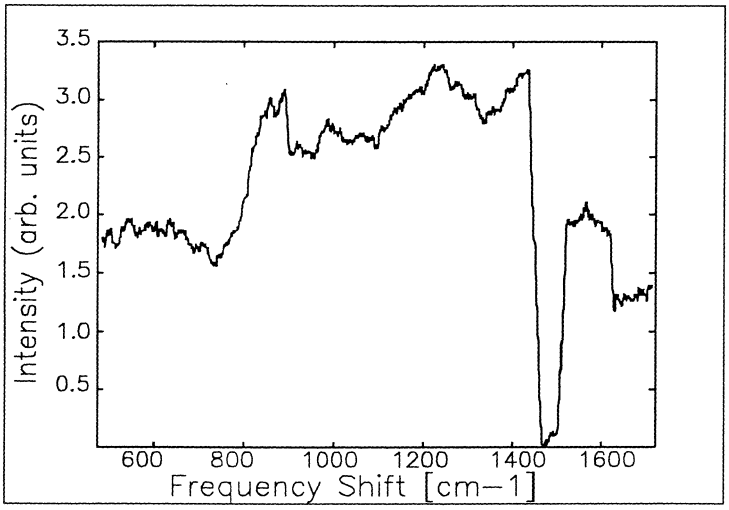

Fig. 6.11. Raman spectra of a Blood clot
(1200 g/mm grating and 500 s integration time)

These spectra show more of a structure than characteristic Raman peaks (nevertheless this structure is reproducible).
The long integration time used in these recordings gave rise to another source of error, namely high signal levels in single channels of the spectra, caused by cosmic radiation. This phenomenon gives sharp peaks in the recorded spectra, which with the shifted-wavelength-technique are integrated up to abrupt "jumps". These "jumps" are especially obvious at 1450 cm^{-1} and 1500 cm^{-1} in the spectrum from a blood clot shown in Fig. 6.11.

7 Optimisation

7.1 Introduction

As mentioned several times throughout this work, the weak nature of Raman scattering puts special demands on the equipment. Also in previous chapters the different parts in the set-up were discussed, including a brief discussion regarding the most suitable choice of equipment for medical use.

To evaluate the further possibilities for diagnostic Raman spectroscopy with this kind of set-up, we will now try to estimate the possible signal gain accomplished by the most suitable equipment available today (January 1996), compared to the set-up used in this work. Other important features such as user friendliness and reliability are also considered. These factors might be difficult to measure in exact figures, but they surely have a great importance in the effective performance and use of the set-up.

7.2 Optimisation of the Set-up

Laser 1: SDL manufactures a diode laser (SDL-5410) able to produce 100 mW (Ref [26]) of single mode light at 800 nm, which is the most powerful single diode laser available in this wavelength region. Around 780 nm several manufactures (SDL, Sony, Sanyo) offer diodes with 50 mW output, which unfortunately seem to be a little bit too weak for Raman spectroscopy on biological materials.

Filters & optics: Collimating optics especially designed for diode lasers (i.e. from Melles Griot (Ref [27])) gives a well-defined focus which simplifies and improves the optical coupling into the fibre bundle. The transmission of such optics is approximately 80% and the coupling efficiency of a well-focused beam is over 50%.

Depending on the sharpness of the laser and the performance of the spectrometer a bandpass filter may or may not be needed. If needed, Kaiser optics offers very narrow holographic bandpass filters with up to 90% transmission (Ref [28]).

This would theoretically give $100*0.8*0.9=72$ mW of light onto the probe and thereby about $0.5*72 \cong 35$ mW output light onto the sample. Compared to the 7 mW in this work the gain is a factor of **5**.

Laser 2: Even more interesting probably the tuneable diode laser array (SDL-8630) also produced by SDL. This laser consists of several weaker laser diodes, but an external cavity stabilises the output beam to a very narrow spectral profile. A manually or computer controlled internal grating gives a 20 nm tuning range, and single mode operation may be achieved at any wavelength according to SDL.

There is also a simpler non-tuneable version of this laser available (SDL-8530), which through temperature and current controlled mode hops is slightly tuneable in the same way as a regular diode laser.

The power output is variable from 0 up to 500 mW in a collimated beam. The external cavity should ensure a narrow base of the laser line so that no bandpass filter is needed. Furthermore, the collimated beam simplifies focusing and coupling into the fibre bundle. This leads to a higher coupling efficiency.

The loss in a single focusing lens (if such a lens is needed) could be neglected and this laser would give 500 mW onto the fibre and thereby approximately 250 mW onto the sample. This means a factor of **35** in gain compared to this work, and although this power might be too high for medical use, it is surely advantageous for experimental purposes.

Probe: In the probe itself there is probably not very much to gain. The arrangement with excitation fibres surrounded by a number of collection fibres is considered as being the most efficient. The crucial point is the optical coupling to and from the fibre bundle. The coupling into the bundle is already discussed and as we shall see, the numerical aperture of the fibres in the bundle plays an important role in the coupling to the spectrometer. Silica-silica fibres from for instance Fiberguide Industries (Ref [30]), has a numerical aperture matching the Kaiser spectrometer described below.

The collection optics: In the ideal case the f-number of the probe will match the spectrometer so that no external optics are needed between the probe and the entrance slit of the spectrometer.

The Spectrometer: The best spectrometer for this purpose is probably the HoloSpec f/1.8i from Kaiser Optical systems (Ref [28]). This spectrometer includes a pre-filtering section for suppressing the Rayleigh-scattered light, which means that the light can be coupled directly from the probe into the spectrometer. If the f/# of the fibres in the probe matches that of the spectrometer the light from a probe end placed in the entrance slit will exactly fill the optics and the grating in the spectrometer. This results in minimal losses and optimal resolution. As all involved optics in this case can be included in the spectrometer and hence would be easy to keep optimally aligned the equipment can be made robust and easy to use.

The spectrometer is based on a holographic grating and lenses instead of a reflecting grating and mirrors used in most spectrometers today. These optical components have very low f/#, which gives a compact spectrometer with a very high optical throughput. The throughput increases with the square of the f/#-ratio. The theoretical gain in our case the would be **5** ($(4/1.8)^2$) in optical throughput and the practical gain in performance and light quality probably worth equally much.

The resolution of the HoloSpec spectrometer is more or less the same as for the Spex spectrometer with the 1200 l/mm grating used in this work, but the spectral coverage is about four times better. According to the manufacture's specification this means 1870 cm^{-1}, (or about 130 nm from 780 nm excitation light) of spectral coverage with a 2 cm^{-1} resolution.

The Detector: A cryogenically-cooled CCD-camera of the type used in this work is without any doubt the only alternative even though the quantum efficiency decreases rapidly above 800 nm for this kind of detector. Nevertheless the use of a so called back-illuminated detector chip would increase the detection efficiency by about a factor of **2** (Ref [29]) resulting in the same gain for the detected Raman-signal.

8 Discussion and Conclusions

8.1 Discussion

As in previous works (Refs [12,13]), high quality Raman spectra were obtained from liquid chemicals such as nitrobenzol. The spectra from strongly fluorescent tissue constitutes show some weak Raman features, while no clear Raman peaks are distinguishable in the spectra from tissue samples. What is then needed to obtain useful, characteristic Raman spectra from biological tissue?

First of all, it has been shown that the Raman signal from normal vessel wall and healthy heart muscle tissue is very weak and featureless. Hydroxyapatite, however, which is formed in advanced atherosclerotic plaque, shows comparatively strong and characteristic Raman signals (Refs [12,13]). Also Cholesterol which is accumulated in the earlier stages of the disorder is comparatively Raman active. Unfortunately no atherosclerotic samples were available for this work.

Secondly, the set-up has to be improved. These matters were discussed in chapter 8 and resulted in a possible theoretical gain in detectable signal levels of **350**!! (35*5*2) or **50** (5*5*2) for the two different laser alternatives.

This might seem like a simplified and optimistic way of calculating, and of course it is, but several practical improvements are then still to be considered. Both the presented laser alternatives give a collimated output beam which is easy to focus and couple into the fibre. A matched coupling from fibre bundle into a spectrometer with an included pre-filtering section instead of an external lens and filter system would yield a better optical quality and less light loss.

The spectra in this work were recorded with up to 500 s integration time and thus these kinds of spectra should be possible to record in seconds. This is almost a complete different time scale, which means much less noise and much less instability in the laser, spectrometer and detector.

Finally, the improved spectral coverage would allow recordings of the whole spectral region from 0 to 1850 cm^{-1} with retained spectral resolution. This would not only decrease the practical recording time with a factor of four compared to this work, but also eliminate changes and inconsistencies as the grating is moved and problems when four spectra have to be put together.

8.2 Conclusions

In this work high quality spectra from chemicals with strong Raman-signal, such as nitrobenzol, were recorded. It is also shown that Raman features are distinguishable even with very short collection times and low laser power.

To get usable recordings from biological materials, however, the set-up obviously has to be substantially improved. The theoretical evaluation shows that the set up indeed can be improved to increase the signal power by at least two orders of magnitude. One can only speculate in the possibilities with such an equipment but clearly there is still a lot to be done in this field.

9 Acknowledgements

I would like to thank my supervisor Stefan Andersson-Engels who have helped me throughout this work.

I am grateful to Claes af Klinteberg who on several occasions helped me to find all kinds of equipment and tools, hidden in various places

Finally I would like to thank Daniela Heinrich and Ulf Gustafsson who always had the time discuss everything that concerned Raman spectroscopy, and a lot of things that did not.

10 References

1 Baraga J J, Feld M S, Rava R P, *Rapid Near-Infrared Raman Spectroscopy of* Human Tissue with a Spectrograph and CCD Detector, Applied Spectroscopy **46**, 187-190, 1992

2 Klug D D, Singleton D L, Walley v M, *Laser Raman Spectrum of Calcified Human Aorta*, Lasers in Surgery and Medicine **12**, 13-17, 1992

3 Redd D C B, Feng Z C,Yue K T, *Gansler T S, Raman Spectroscopic Characterization of Human Breast Tissue: Implications for Breast Cancer Diagnosis*, Applied Spectroscopy **47**, 787-791, 1993

4 Clarke R H, Wang Qian, Isner J M, *Laser Raman Spectroscopy of atherosclerotic lesions in homan coronary artery segments*, Applied Optics **27**, 4799-4800, 1988

5 Clarke R H, Hanlon E B, Isner J M, Brody H, *Laser Raman Spectroscopy of calcified atherosclerotic in cardiovascular tissue*, Applied Optics **26**, 3175-3177, 1987

6 Newton I, *Optics*, 4th ed. reprint. London: Bell, 1931

7 Fraunhofer J, *Ann. d. Physik* **56-264** 1817 (Ames J S Prismatic and Diffraction Spectra), New York: Harper and Brothers 1899

8 Kirhoff G R, *Monatsber. d. Ber. Akad. d. Wiss*, 1859 pp.783-787; *Ann. d. Physic*, **109, 148, 245,** 1860; *Phil. Mag.*, **20**, 1860; *Ann. Chim. Physique*, **58, 254**,1860

9 Sawyer R A, *Experimental Spectroscopy*, New York: Dover Publications Inc., 1963

10 Svanberg S, *Atomic and Molecular Spectroscopy*, Berlin Heidelberg: Springer-Verlag,1991

11 More L T, *Isaac Newton*, New York: Charles Screibner's Sons, 1934

12 Gustafsson U, *Near-Infrared Raman Spectroscopy Usinng a Diod Laser and CCD-Detector for Tissue Diagnostics*, Lund Reports on Atomic Physics LRAP-**138**, 1993

13 Bood J, Carlsson H, *Raman and Infrared Absorption Spectroscopy for Tissue Diagnostics*, Lund Reports on Atomic Physics LRAP-**168**, 1995

14 Haken H, Wolf C H, *The Physics of Atoms and Quanta*, Third Edition, Springer Verlag, Heidelberg, 1993

15 Cheng D K, *Field and Wave Electromagnetics*, Second Edition, Addison-Wesley publishing Company, 1993

16 Colthup N B, Daily L H, Wiberly S E, *Introduction to Infrared and Raman Spectroscopy*, Academic Press, San Diego, 1990

17 Nishimura Y, Mirakawa A Y, Tsuboi M, *Resonance Raman Studies of Nuclei Acids*, Advances in Infrared and Raman Spectroscopy **5**, 217-275, 1978

18 Dollish F R, Fateley W G, Bentley F F, *Characteristic Raman Frequencies of Organic Compounds*, Jonh Wiley & Sons, Toronto, 1974

19 Andrsson-Engels Stefan, *Laser-Induced Fluorescence fo Medical Diagnostics*, Lund Reports on Atomic Physics LRAP-**108**, 1989

20 Svanberg K, *Fluorescence Diagnosis of Tumours and Atherosclerotic Lesions and Photochemical Treatment*, Lund University Hospital, Lund, 1989

21 Lindod G, *Blood Vessels and Lymphatics, in Andersson J R (ed.), Muir's Textbook of Pathology*, Edward Arnold, London, 1992

22 Schoen F J, *Blood Vessels*, in Robbins (ed.), *Pathologic Basis of Disease*, 5th edition W. B. Saunders Company, 1994

23 Benditt E P & Schwartz S M, *Blood Vessels*, in Rubin & Former, *Pathology*, 2:nd edition J. B. Lippincoff Cmpany 1994

24 Svanberg S, *Tissue Diagnostics Using Lasers*, Chapter7 in Pettit G & Wayant R W (ed) *Lasers in Medicine*, Plenum, New York

25 Faiman R, *Raman Spectroscopic Studies of Dífferent Forms of Cholesterol and its Derivates in the Crystaline State,* Chemistry and Physics of Lipids **18**, 84-104, (1977)

26 SDL, *Product Catalogue* 1995

27 Melles Griot, *Product Catalogue* 1995

28 Kaiser Optical Systems, *Product Catalogue* 1995

29 Princeton Instruments, *Product Catalogue* 1995

30 Fiberguide Industries, *Product Catalogue* 1995

31 Raman C V & Krishnan K S, *A New Type of Secondary Radiation*, Nature **121**, 501-502, 1928

32 Raman C V & Krishnan K S, *A Cange of Wave-length in Light Scattering*, Nature **121, 619**, 1928

33 Raman C V & Krishnan K S, *The Optical Analogue of the ComtonEffect*, Nature **121, 711**, 1928

34 Frank C J, McCreery R L, Redd D C B, Gansler T S, *Detection of Silicon in Lymph Node Biopsy Speciments by Near-Infrared Raman Spectroscopy*, Applied Spectroscopy **47**, 387-390, 1993

35 Newman C D, Bret G G, McCreery R L, *Fiber-Optic Sampling Compined with an Imaging Spectrograph for Routine Raman Spectroscopy*, Applied Spectroscopy **46**, 262-264, 1992

36 Williamson J M, Bowling R J, McCreery R L, *Near-Infrared Raman Spectroscopy with a 783 nm Diod Laser and CCd Array Detector*, Applied Spectroscopy **43**, 372-375, 1990

37 Allred C D, McCreery R L, *Near-Infrared Raman Spectroscopy of Liquids and Solids with a Fiber-Optic Sampler and CCD Detector*, Applied Spectroscopy **44**, 1229-1231, 1990

Appendix A-Basic Physics, Energy levels and Units

Quantum Mechanics

In a quantum-mechanical world electro-magnetic radiation, in daily talk light, is no longer seen as continuos flow, but as a stream of energy quanta, photons.
The photons are characterised by their energy E, which is associated with the light wavelength λ according to:

$$\lambda = \frac{hc}{E}$$

Here c and h are constants known as velocity of light and Plank's constant.
The human eye, which can only detect a small part of the wavelength-spectra, interprets different wavelengths as different colours.

These photons can be created or annihilated in interaction with atoms or molecules in the surrounding media. As one of the most fundamental laws in physics states that energy cannot be created or destroyed, this interaction must be in the form of transference of energy from the media to the photon, or vice versa.

Classically an atom consists of a core surrounded by a cloud of electrons. Quantum-mechanics says that these electrons only can exist in well-defined orbits, each with a discrete quantified energy, so called energy-levels.

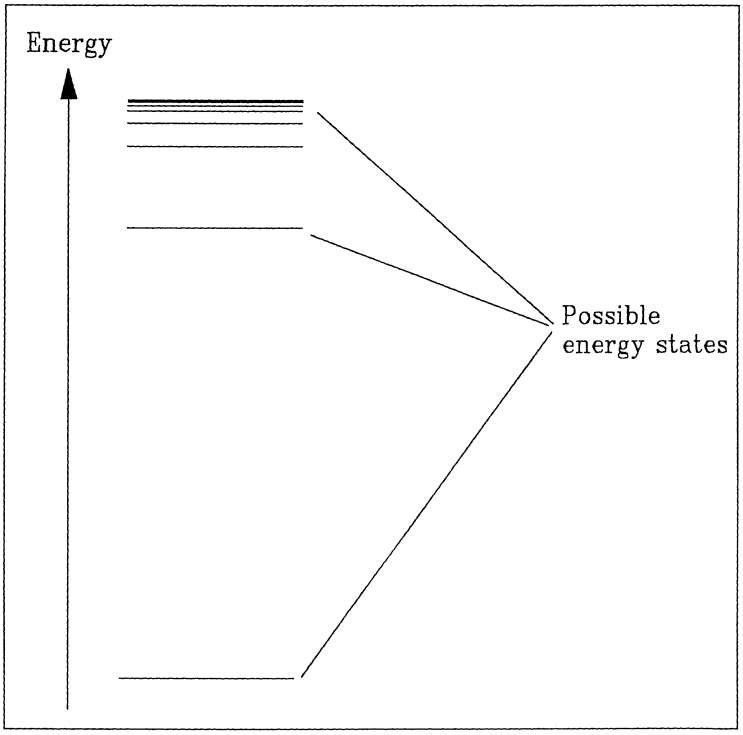

Fig. A1 Energy levels in a hydrogen atom

If a photon with an energy that exactly fits the gap between two levels interacts with an atom, the energy can be transferred to the atom which is excited to a higher energy-level, while the photon is annihilated.

Under normal circumstances (normal temperature, pressure, etc.), the only stable state for an atom is the lowest possible which is called the ground-state. Therefore the atom returns to this level by creating a new photon, emitted in an arbitrary direction.

In a molecule, built of several atoms, the situation is very much the same, but rotation and vibration give rise to further possibilities of energy states, resulting in a more complex set of levels for the total energy of the molecule.

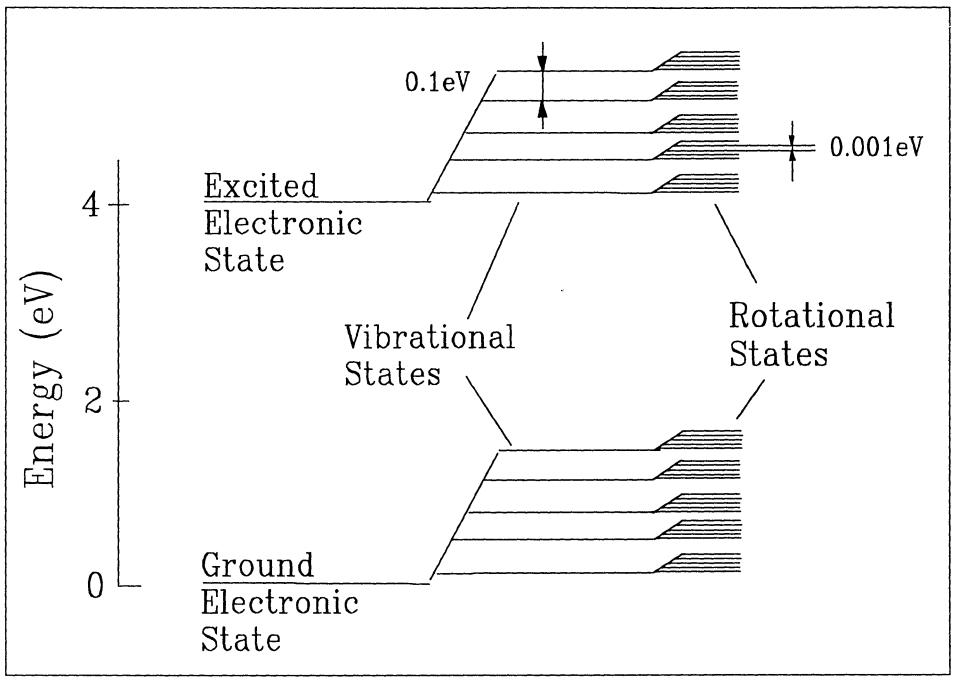

Fig A2 Energy levels of a molecule. (From Ref. [10])

Units

Most of the mathematics in this work involves light, or photons. In today's physics light is considered to have a double-nature. It can be seen either as an "energy-particle", a so called photon, or as a wave-movement. Closest to reality is probably to say that it is both. This means that light is associated with wavelength, frequency and velocity as any wave movement but also with a quantified energy and other particle properties. (It is for instance possible to count single photons)
The different properties are labelled and connected as follows:

Property	**Label**	**Unit**
Wavelength	λ	(nm)
Frequency	υ	(Hz)
Energy	E	(eV)
Velocity of light	c	(m/s)
Plank's constant	h	(eVs)
Wavenumber	σ	(cm^{-1})

$$\sigma = \frac{1}{\lambda}$$

$$c = \lambda\upsilon$$

$$E = h\upsilon$$

$$\Rightarrow E = \frac{hc}{\lambda}$$

Notable is that the light is described equally well by its energy, wavelength, frequency or wavenumber and that one easily converts between the different units. Which one to use is then only a matter of convenience and normally depends on conventions within the specific subject of physics. Raman spectroscopists normally use wavenumbers.

For further reading on atomic physics Ref. [10] is recommended.. The spectroscopic aspects of energy-levels and light-matter interaction are discussed in Ref. [14].

Appendix B-Matlab files

aafit.m

```
% Define variables
        base=zeros(N,1);
        fitted=zeros(N,1);
        xaxis=1:1:N;

% Fit curve
        Fit=polyfit(x,curve,2);
        for i=1:N
          base(i)=xaxis(i)^2*Fit(1)+xaxis(i)*Fit(2)+Fit(3);
        end

% Subtract base
        for i=1:N
          fitted(i)=curve(i)-base(i);
        end
```

aadif.m

```
% Define variables
        Int=zeros(N,1);

%Calibration
        S1Sum=sum(S1);
        for i=1:N
          S1(i,1)=S1(i,1)/S1Sum;
        end
        S2Sum=sum(S2);
        for i=1:N
          S2(i,1)=S2(i,1)/S2Sum;
        end

%Diferentiation
        Diff=S1(1:N,1)-S2(1:N,1);

%Integration
        for i=2:N
          Int(i,1)=Diff(i,1)+Int((i-1),1);
        end
```

Appendix C-Raman shifts of Cholesterol

Observed Raman shifts of Cholesterol

Ref [13]	Ref [25] Cholesterol monohydrate	Ref [25] Anhydrous cholesterol
541	545 s	550 s
600	603 vs	600 s
695		693 vs
	700 vs	
798	803 s	
	846 vs	
874		
915	885 s	
957	960 s	
1003		
		1068 s
1081	1088 s	
1126	1132 vs	
1171		
		1300 s
	1326 vs	1328 s
1444	1448 vs	1444 vs
		1468 vs
1669		1668 vs
	1673 vs	